Electron Affinities of Silicon Hydrides: SiH_n ($n = 0-4$) and Si_2H_n ($n = 0-6$)

Chaeho Pak, Jonathan C. Rienstra-Kiracofe, and Henry F. Schaefer, III*

Contribution from the Center for Computational Quantum Chemistry, University of Georgia, Athens, Georgia 30602-2525

Received: August 22, 2000

The molecular structures and electron affinities of the SiH_n/SiH_n^- ($n = 1-4$) and $Si_2H_n/Si_2H_n^-$ ($n = 0-6$) molecules, as well as the silicon atom, have been investigated using density functional theory (DFT) and hybrid Hartree−Fock/density functional theory. Specifically, four different types of electron affinities are reported in this work: the adiabatic electron affinity (EA_{ad}), zero-point corrected EA_{ad} (EA_{zero}), the vertical electron affinity (EA_{vert}), and vertical detachment energy (VDE). The basis set used in this work is of double-ζ plus polarization quality with additional s- and p-type diffuse functions, and is denoted as DZP^{++}. Of the six different density functionals used in this work, the BHLYP functional predicted the best molecular structures, and the B3LYP functional predicted the best electron affinities. When compared to the available six experimental electron affinities, the B3LYP functional has an average absolute error of just 0.06 eV. We predict the unknown electron affinities for Si_2H_2 (dibridged), Si_2H_3, Si_2H_4 (disilene), and Si_2H_5 (disilyl radical) to be 0.45, 2.21, 1.34, and 1.85 eV, respectively. These predictions assume that the (unknown) molecular structure of each anion is analogous to the known structure of the corresponding neutral molecule. The most interesting aspect of the present research is that for $Si_2H_2^-$ and $Si_2H_4^-$, the lowest energy structures are qualitatively different from those of the neutrals. For $Si_2H_2^-$ the disilavinylidene structure H_2SiSi^-, is predicted to lie 24 kcal/mol below the dibridged or "butterfly" anion. For $Si_2H_4^-$ the silylsilylene anion H_3SiSiH^-, is predicted to lie 3 kcal/mol below the disilene anion structure $H_2SiSiH_2^-$. The zero-point corrected adiabatic electron affinities of disilavinylidene, silylsilylidyne, and silylsilylene are 1.87, 1.01, and 1.71 eV, respectively. The saturated closed shell systems SiH_4 and Si_2H_6 do not have conventional electron affinities.

Introduction

Silicon, like its first row counterpart, carbon, is a chemist's cornucopia.[1] The ability of silicon to make one, two, three, four, and even five-coordinate compounds is one of the primary reasons for its inexhaustible chemistry.[1] Among the simplest silicon species are the silicon hydrides, SiH_n ($n = 0-4$) and Si_2H_n ($n = 0-6$). Silicon hydrides play an important role in silicon chemical vapor deposition (CVD) processes,[2] which are of great significance to the semiconductor industry. Because of this significance, numerous experimental[3−17] and theoretical[18−36] studies have examined various chemical properties of the silicon hydrides, their corresponding ions, and other simple silicon-based compounds.

Silicon hydride systems are also of interest to chemists because of their sometimes unique bonding characteristics when compared to their simple hydrocarbon analogues. Although analogous carbon and silicon species are isovalent, the chemical properties of carbon and silicon congeners can be quite different. One of the reasons for these differences is that the relative orbital sizes of the valence s and p orbitals are different for the carbon and silicon atoms; silicon has a larger p orbital than carbon, and carbon has a larger *s* orbital than silicon.[37,38] Many properties of the species in the SiH_n/SiH_n^- ($n = 0-4$) and $Si_2H_n/Si_2H_n^-$ ($n = 0-6$) series may be compared to their carbon analogues, and some interesting differences may be found, for example, by comparing the adiabatic electron affinities of simple silicon hydrides to their hydrocarbon analogues.

In this work, we investigate the electron affinities (EA) of the silicon hydrides and the ability of density functional theory to predict accurate electron affinities for these species through comparisons to known experimental EAs and analogous hydrocarbon EAs. Experimental EAs[4,7,10,13,14] are available for Si, SiH, SiH_2, SiH_3, Si_2, and Si_2H.

When predicting molecular energies, structures, and electron affinities, there are many theoretical approaches, but considering both reliability and computational expense, gradient corrected density functional theory (DFT) has been shown to be effective for predicting EAs of many inorganic species such as the SiF_n/SiF_n^-, SF_n/SF_n^-, PF_n/PF_n^-, ClF_n/ClF_n^-, $C_2F_n/C_2F_n^-$, and BrF_n/BrF_n^- series.[31,39−43] In addition, while the theoretical prediction of an electron affinity is generally difficult due to the result being a small difference between two very large energies, our previous work has shown that DFT can be a dependable source for electron affinity predictions,[44−47] when used in a knowledgeable manner.

Methods

Six different density functional or hybrid Hartree−Fock/density functional methods were used in this study. Five are gradient corrected functionals: Becke's 1988 exchange functional[48] (B) with Lee, Yang, and Parr's correlation functional[49] (LYP), BLYP; Becke's half-and-half exchange functional[50] (BH) with the LYP correlation functional, BHLYP; Becke's three-parameter exchange functional[51] (B3) with the LYP correlation functional, B3LYP; the B exchange functional with the Perdew correlation functional[52] (P86), BP86; and the B3 exchange functional with the P86 correlation functional B3P86. The sixth density functional scheme used in this study was the standard local-spin-density approximation (LSDA) which employs the 1980 correlation functional of Vosko, Wilk, and Nusair[53] along with Slater's exchange functional.[54] The unrestricted Kohn−Sham method was used for all closed and open shell systems.[55]

10.1021/jp003029y CCC: $19.00
Published on Web 11/05/2000

All computations have been evaluated with the Gaussian 94 program suite.[56] Using the default integration grid (75 302), the integrals that are evaluated in this study should be accurate to 1×10^{-5} E_h. The Kohn−Sham density was converged to $1 \times 10^{-8} E_h$ and Cartesian gradients were converged to at least 10^{-6} au.

A standard double-ζ plus polarization (DZP) basis set with the addition of diffuse functions was utilized. The DZ part of the basis set was constructed from the Huzinage−Dunning-Hay[57] set of contracted Gaussian functions. The DZP basis was formed by the addition of a set of five d-type polarization functions for Si and a set of *p*-type polarization functions for H [$\alpha_d(Si) = 0.50$, $\alpha_p(H) = 0.75$]. The DZP basis was augmented with diffuse functions; Si received one additional s-type and one additional set of p-type functions, and H received one additional s-type function. The diffuse function orbital exponents were determined in an "even-tempered sense" as a mathematical extension of the primitive set, according to the formula of Lee and Schaefer[58] [$\alpha_s(Si) = 0.02729$, $\alpha_p(Si) = 0.02500$, $\alpha_s(H) = 0.04415$]. The final contraction scheme for this basis is Si (12s8p1d/7s5p1d) and H (5s1p/3s1p).

The geometries reported in Figures 1−14 were found to be minima after determining the harmonic vibrational frequencies via analytic gradients at the corresponding stationary point structures of each functional.

Finally, for SiH and SiH^-, we have performed coupled cluster studies with all single and double excitations and perturbative nonconnected triple excitations [CCSD(T)],[59−61] to verify experimental data. The basis set used for the CCSD(T) computation was the correlation-consistent polarized valence quadruple-ζ set of Dunning[62,63] augmented with diffuse functions and is denoted aug-cc-pVQZ. An ROHF reference was used and core electrons for Si were frozen during CCSD(T) energy computations. These computations were done using ACES II ab initio program system.[64]

Electron affinities are evaluated as a difference in total energies in the following manner: the classical adiabatic electron affinities are determined by

$$EA_{ad} = E_{(\text{optimized neutral})} - E_{(\text{optimized anion})}$$

zero-point corrected adiabatic electron affinities are determined by

$$EA_{zero} = E_{(\text{zero-point corrected neutral})} - E_{(\text{zero-point corrected anion})}$$

the vertical electron affinities by

$$EA_{vert} = E_{(\text{optimized neutral})} - E_{(\text{anion at neutral equilibrium geometry})}$$

and the vertical detachment energy by

$$VDE = E_{(\text{neutral at anion equilibrium geometry})} - E_{(\text{optimized anion})}$$

Note that in many cases theoretical EA_{ad} values are closer to experimental electron affinities than EA_{zero} values, despite the fact that experimental values are truly EA_{zero}.[44−47] This effect may be due to errors in a harmonic approximation to zero-point vibrational energy; however, the corrections for zero-point vibrational energies are always relatively small, and thus unimportant in terms of our overall results.

Results

The electron affinity for the Si atom is given in Table 1. All four electron affinities for SiH_n ($n = 1-4$) and Si_2H_n ($n = 0-6$) are reported in Tables 2 and 3, respectively. Optimized geometries for each molecular species with all functionals are shown in Figures 1−14.

TABLE 1: Electron Affinity of Si in eV (kcal/mol in Parentheses)

method	EA
B3LYP	1.36(31.4)
B3P86	1.99(45.9)
BHLYP	1.18(27.1)
BLYP	1.24(28.6)
BP86	1.57(36.3)
LSDA	2.01(46.5)
exptl[a]	1.389521 ± 0.00002(32.0)

[a] Reference 14.

A. Si and Si^-. The electron affinities of the Si (^3P) atom with various functionals, as well as the experimental electron affinity are reported in Table 1. All six functionals predict the electron affinity of the Si atom within a deviation of at most 0.62 eV (LSDA) from experiment. As is the case for most atomic systems,[47] B3LYP predicts the best electron affinity for Si. In this instance, the electron affinity was 0.03 eV lower than the experimental value, given by Scheer, Bilodeau, Brodie, and Haugen's single and multiphoton tunable infrared laser experiments.[14] We note here that carbon and silicon have similar electron affinities from experiment;[14] C = 1.262 eV, Si = 1.389 eV and that B3LYP and BLYP are within 0.15 eV for both silicon and carbon.[47]

B. SiH and SiH^-. Theoretical equilibrium geometries of silylidyne (silicon monohydride), SiH ($X\ ^2\Pi$), and its anion, SiH^- ($X\ ^3\Sigma^-$) are displayed in Figure 1. The experimental r_e of neutral silylidyne is 1.5201 Å.[65] Comparing with the experimental value, the most accurate bond length was predicted by BHLYP, being only 0.008 Å shorter than experiment. The hybrid functionals (B3LYP, B3P86, BHLYP) are within ± 0.013 Å of experiment, while the pure functionals (BLYP, BP86, LSDA) overestimate experiment by at least 0.026 Å. All functionals give a longer bond length for the anion than the neutral, by about 0.03 Å on average. In 1975, Kasdan, Herbst, and Lineberger[4] estimated the experimental r_e of the anion at 1.474 ± 0.004 Å which is 0.09 Å shorter than our average bond length of 1.565 Å. In 1978, Rosmus and Meyer[66] reinterpreted the laser photoelectron data of Kasdan et al. and found r_e (SiH^-) = 1.566 ± 0.004 Å with a ω_e (SiH^-) = 1804 cm^{-1}. Both the original and revised values are based on a Badger's rule estimate, and early theoretical results[66−68] supported the revised values. Our DFT results also predict r_e of the anion in good agreement with the revised experimental results.

To further investigate this matter, we performed CCSD(T)/aug-cc-pVQZ computations on SiH and SiH^-. We obtain r_e (SiH) = 1.524 Å and r_e (SiH^-) = 1.553 Å, along with ω_e (SiH) = 2043 cm^{-1} and ω_e (SiH^-) = 1860 cm^{-1}. The theoretical neutral bond length is just 0.004 Å longer than experiment and the harmonic frequency is only 1 cm^{-1} greater than the experimental ω_e = 2042 cm^{-1}. Furthermore, previous UCCSD(T)/aug-cc-pV5Z calculations[34] predict r_e (SiH) = 1.522 Å. Our r_e (SiH^-) is 0.013 Å shorter than Rosmus and Meyer's revised value. Because the original experiment did not directly deduce ω_e, an error of ~50 cm^{-1} in the determination of ω_e can be expected.[4] We therefore suggest that the true r_e and ω_e for SiH^- are within ± 0.01 Å and ± 40 cm^{-1} of our CCSD(T)/aug-cc-pVQZ values. As with SiH, the hybrid functionals predict the best r_e for SiH^-, being within ± 0.008 Å of the CCSD(T) value, while the pure functionals overestimate the CCSD(T) result by at least 0.019 Å.

The EA_{ad} with CCSD(T) is 1.248 or 1.259 eV with ZPVE correction, and is only 0.029 or 0.018 (with ZPVE) eV lower

TABLE 2: The Adiabatic Electron Affinity (EA_{ad}), Zero-Point Corrected EA_{ad} (EA_{zero}), Vertical Electron Affinity (EA_{vert}), and the Vertical Detachment Energy (VDE) for SiH_n ($n = 1-4$) Species, Presented in eV (kcal/mol in Parentheses)

species	method	EA_{ad}	EA_{zero}	EA_{vert}	VDE
SiH	B3LYP	1.28(29.6)	1.30(29.9)	1.28(29.5)	1.29(29.7)
	B3P86	1.89(43.7)	1.90(43.9)	1.89(43.6)	1.90(43.8)
	BHLYP	1.11(25.6)	1.12(25.9)	1.11(25.5)	1.12(25.8)
	BLYP	1.16(26.8)	1.17(27.0)	1.16(26.7)	1.17(26.9)
	BP86	1.48(34.0)	1.49(34.3)	1.47(33.9)	1.48(34.1)
	LSDA	1.89(43.7)	1.90(43.9)	1.89(43.6)	1.90(43.8)
	CCSD(T)	1.248(28.8)	1.259(29.0)		
	exptl[a]		1.277 ± 0.009		1.276 ± 0.006
SiH_2	B3LYP	1.17(27.0)	1.20(27.6)	1.16(26.8)	1.18(27.3)
	B3P86	1.76(40.7)	1.79(41.2)	1.75(40.4)	1.77(40.9)
	BHLYP	1.00(23.2)	1.03(23.8)	0.99(22.9)	1.02(23.5)
	BLYP	1.05(24.3)	1.08(24.8)	1.04(24.0)	1.06(24.5)
	BP86	1.34(31.0)	1.37(31.5)	1.33(30.8)	1.35 (31.2)
	LSDA	1.74(40.1)	1.76(40.6)	1.73(39.9)	1.75(40.3)
	exptl[b]		1.124 ± 0.020		1.124 ± 0.003
SiH_3	B3LYP	1.40(32.2)	1.45(33.4)	0.96(22.0)	1.91(44.0)
	B3P86	1.89(43.5)	1.94(44.7)	1.43(32.9)	2.42(55.9)
	BHLYP	1.17(26.9)	1.22(28.1)	0.72(16.5)	1.68(38.8)
	BLYP	1.31(30.3)	1.37(31.5)	0.84(19.4)	1.81(41.8)
	BP86	1.49(34.5)	1.55(35.7)	1.05(24.3)	2.02(46.6)
	LSDA	2.02(46.5)	2.06(47.6)	1.57(36.3)	2.55(58.7)
	exptl[c]		1.406 ± 0.014		
SiH_4	B3LYP	−0.74(−17.0)	−0.73(−16.8)	−0.74(−17.0)	−0.74(−17.0)
	B3P86	−0.32(−7.3)	−0.30(−7.0)	−0.32(−7.3)	−0.32(−7.3)
	BHLYP	−0.91(−21.1)	−0.91(−21.0)	−0.91(−21.1)	−0.91(−21.1)
	BLYP	−0.80(−18.4)	−0.79(−18.2)	−0.80(−18.4)	−0.80(−18.4)
	BP86	−0.64(−14.7)	−0.62(−14.4)	−0.64(−14.7)	−0.63(−14.6)
	LSDA	−0.28(−6.5)	−0.26(−6.1)	−0.28(−6.5)	−0.28(−6.4)

[a] Reference 4. [b] Reference 4. [c] Reference 7.

than the experimental[4] laser photoelectron value of 1.277 ± 0.009 eV. As with Si, the best DFT electron affinity for SiH was predicted by B3LYP, which value is close (better than 0.03 eV) to experiment for both EA_{vert} and EA_{zero}. Other functionals gave electron affinity results within $\pm$ 0.2 eV, except for LSDA and B3P86. (See Table 2.)

The electron affinity[69] of CH is similar to the electron affinity of SiH,[4] 1.238 eV vs 1.277 eV. Density functional theory also describes EA_{ad} (CH) well,[47] though our results for EA_{ad} (SiH) are about 0.1 eV better on average.

C. SiH_2 and SiH_2^-. Our optimized geometries for silylene, SiH_2 ($\tilde{X}\ ^1A_1$) and SiH_2^- ($\tilde{X}\ ^2B_1$) are shown in Figure 2. The three hybrid functionals are within $\pm$ 0.014 Å of the experimental[70] SiH_2 r_0 value, while the pure functionals overestimate experiment by at least 0.014 Å. All functionals are within 1.1° of the experimental angle, except LSDA. Our results for the neutral species are similar to the recent UCCSD(T)/aug-cc-pV6Z results of 1.516 Å and 92.3°.[34] We observe little change in the HSiH angle between SiH_2 and SiH_2^-, in accordance with the Walsh picture for the valence b_1 molecular orbital in XH_2 molecules. The bond lengths in SiH_2^- are about 0.02 Å longer than the neutral. Compared to methylene, CH_2, the electronic states for the anions ($^2B_1$) are the same, but states for the neutral species are different: the ground state for methylene is $^3B_1$ vs $^1A_1$ in silylene. Predicted geometries and electron affinities with DFT for SiH_2 and SiH_2^- should be more accurate than for CH_2,[47] which has large multireference character in its wave function due to the near degeneracy of the valence a_1 and b_1 molecular orbitals.

Our theoretical EA_{ad}, EA_{zero}, EA_{vert}, and VDE for SiH_2 are listed in Table 2. The predicted EA_{ad} ranges from 1.00 to 1.74 eV, among which BHLYP predicts the lowest EA_{ad}. The BHLYP EA_{ad} and EA_{vert} are often lower than those obtained with the other functionals, as is the case in many inorganic fluoride series.[39-43] Because there is not much difference in geometries between the neutral and the anion, the differences with a given functional between EA_{ad}, EA_{zer}, EA_{vert}, and VDE are small. From Leopold et al.,[71] CH_2 has an experimental electron affinity of 0.652 eV compared to Kasdan, Herbst, and Lineberger's laser photoelectron spectrometry results for SiH_2 of 1.124 ± 0.020 eV.[4] The large difference in EAs for methylene and silylene is due to the fact that the extra electron must add to a singly occupied a_1 orbital in CH_2, but adds to a unoccupied, nonbonding b_1 orbital in SiH_2. For SiH_2, B3LYP, BLYP, and BHLYP EA_{zero} values are within $\pm$ 0.09 eV of experiment; remarkably in CH_2, B3LYP, BLYP, and BP86 are within 0.14 eV of experiment. However, BHLYP suffers from Hartree−Fock deficiencies, predicting an EA 0.35 eV lower for the multireference described CH_2.[47]

D. SiH_3 and SiH_3^-. The C_{3v} symmetry equilibrium geometries of the SiH_3 ($\tilde{X}\ ^2A_1$) radical and SiH_3^- ($\tilde{X}\ ^1A_1$) anion are shown in Figure 3. The neutral, silyl radical bond lengths ranged from 1.474 (BHLYP) to 1.496 (BP86) Å, and the bond angles from 111.1° to 111.4°. All methods overestimate the experiment values[72] of 1.468 Å and 110.5°. However, our results are much closer to the UCCSD(T)/aug-cc-pVQZ values[34] of 1.482 and 111.3°. The anion bond distances are significantly longer, 1.532 to 1.558 Å, and the angles are tighter, 93.8° to 96.0°. This is in agreement with an experimentally observed tightening from ~112.5° to ~94.5° between the neutral species and the anion.[7] Our hybrid functional bond lengths for the anion are just $\pm$ 0.007 Å from the BS1 CCSD(T)-R12 results, $r_{(Si-H)} = 1.538$ Å, obtained by Aarset et al.[36] The pure functionals overestimate the CCSD(T) result by at least 0.14 Å. All bond angles are in reasonable agreement with the BS1 CCSD(T)-R12 bond angles of 95.196°.

The best electron affinity result was from the B3LYP level of theory, $EA_{ad} = 1.40$ eV, which is 0.01 eV lower than that determined by photoelectron spectroscopy,[7] 1.406 ± 0.014 eV, though agreement is slightly worse with the ZPVE correction.

TABLE 3: The Adiabatic Electron Affinity (EA_{ad}), Zero-point Corrected EA_{ad} (EA_{zero}), Vertical Electron Affinity (EA_{vert}), and the Vertical Detachment Energy (VDE) for Si_2H_n ($n = 0-6$) Species, Presented in eV (kcal/mol in Parentheses)

species	method	EA_{ad}	EA_{zero}	EA_{vert}	VDE
Si_2	B3LYP	2.06(47.5)	2.05(47.4)	1.86(42.9)	2.28(52.6)
	B3P86	2.65(61.2)	2.65(61.1)	2.44(56.4)	2.89(66.6)
	BHLYP	1.79(41.3)	1.78(41.1)	1.60(36.9)	2.00(46.1)
	BLYP	1.98(45.6)	1.97(45.4)	1.77(40.8)	2.08(47.9)
	BP86	2.28(52.6)	2.27(52.4)	2.07(47.6)	2.28(52.7)
	LSDA	2.90(66.8)	2.89(66.7)	2.66(61.3)	3.16(72.8)
	exptl[a]		2.202 ± 0.010		
Si_2H ($^2B_1 \leftarrow {}^2A_1$)	B3LYP	2.27(52.3)	2.26(52.1)	2.22(51.2)	2.31(53.3)
	B3P86	2.86(65.8)	2.85(65.6)	2.81(64.8)	2.90(66.9)
	BHLYP	2.08(48.0)	2.07(47.8)	2.04(47.0)	2.13(49.1)
	BLYP	2.13(49.0)	2.12(48.9)	2.08(48.0)	2.17(50.1)
	BP86	2.42(55.8)	2.41(55.6)	2.37(54.7)	2.46(56.8)
	LSDA	3.00(69.1)	2.99(68.9)	2.95(68.0)	3.05(70.3)
Si_2H ($^2A_1 \leftarrow {}^1A_1$)	B3LYP	2.31(53.2)	2.31(53.3)	2.30(53.1)	2.31(53.3)
	B3P86	2.86(66.0)	2.87(66.1)	2.86(65.8)	2.90(66.9)
	BHLYP	2.20(50.8)	2.21(50.9)	2.20(50.7)	2.13(49.1)
	BLYP	2.13(49.0)	2.13(49.1)	2.12(48.8)	2.17(50.1)
	BP86	2.38(54.8)	2.38(54.9)	2.37(54.6)	2.46(56.8)
	LSDA	2.87(66.2)	2.87(66.2)	2.86(65.9)	3.05(70.3)
	exptl[b]		2.31 ± 0.10		
Si_2H_2 (dibridged)	B3LYP	0.34(7.7)	0.45(10.4)	0.23(5.3)	0.47(10.8)
	B3P86	0.91(21.0)	1.01(23.4)	0.80(18.5)	1.04(24.0)
	BHLYP	0.06(1.4)	0.18(4.1)	−0.04(−0.9)	0.18(4.2)
	BLYP	0.29(6.8)	0.38(8.7)	0.18(4.3)	0.44(10.1)
	BP86	0.57(13.1)	0.65(14.9)	0.46(10.6)	0.70(16.2)
	LSDA	0.93(21.5)	1.00(23.1)	0.83(19.0)	1.07(24.6)
Si_2H_3	B3LYP	2.21(51.0)	2.21(51.0)	2.09(48.2)	2.28(52.7)
	B3P86	2.78(64.1)	2.78(64.1)	2.65(61.1)	3.65(84.3)
	BHLYP	2.00(46.0)	1.99(45.9)	1.88(43.4)	2.91(67.1)
	BLYP	2.09(48.1)	2.09(48.2)	1.93(44.5)	2.16(49.9)
	BP86	2.35(54.3)	2.35(54.3)	2.18(50.3)	2.43(56.1)
	LSDA	2.92(67.4)	2.92(67.3)	2.68(61.9)	3.02(69.7)
Si_2H_4 (disilene)	B3LYP	1.28(29.5)	1.34(31.0)	0.58(13.5)	1.80(41.4)
	B3P86	1.83(42.2)	1.89(43.6)	1.08(24.9)	2.37(54.6)
	BHLYP	1.16(26.8)	1.23(28.4)	0.28(6.4)	1.75(40.3)
	BLYP	1.13(25.9)	1.19(27.4)	0.54(12.5)	1.59(36.7)
	BP86	1.36(31.4)	1.42(32.8)	0.74(17.1)	1.85(42.7)
	LSDA	1.68(38.8)	1.74(40.1)	1.01(23.3)	2.19(50.6)
Si_2H_5 (disylyl radical)	B3LYP	1.80(41.5)	1.85(42.7)	1.20(27.6)	2.46(56.8)
	B3P86	2.32(53.5)	2.37(54.6)	1.70(39.1)	3.01(69.4)
	BHLYP	1.56(36.0)	1.61(37.2)	0.96(22.1)	2.22(51.3)
	BLYP	1.71(39.5)	1.77(40.8)	1.11(25.7)	2.37(54.6)
	BP86	1.92(44.3)	1.97(45.5)	1.30(30.1)	2.60(60.1)
	LSDA	2.46(56.6)	2.50(57.6)	1.84(42.4)	3.16(72.8)
Si_2H_6	B3LYP	−0.61(−14.1)	−0.53(−12.3)	−0.63(−14.5)	−0.59(−13.5)
	B3P86	−0.16(−3.7)	−0.08(−1.8)	−0.18(−4.1)	−0.13(−3.0)
	BHLYP	−0.88(−20.4)	−0.83(−19.2)	−0.89(−20.6)	−0.87(−20.2)
	BLYP	−0.61(−14.0)	−0.50(−11.6)	−0.63(−14.6)	−0.56(−13.0)
	BP86	−0.42(−9.8)	−0.32(−7.4)	−0.49(−10.4)	−0.38(−8.8)
	LSDA	−0.08(−1.8)	0.05(1.0)	−0.11(−2.6)	−0.02(−0.5)

[a] Reference 10. [b] Reference 13.

The EA_{vert} ranged from 0.72 to 1.57 eV and the VDE ranged from 1.68 to 2.55 eV. It is interesting to note that the electron affinity of the methyl radical,[73] where the neutral species is D_{3h} ($^2A_2''$), is only 0.08 eV compared to 1.406 eV for the silyl radical.[7] B3LYP and BLYP both predict EA (CH_3) to within 0.05 eV.[74]

E. SiH_4 and SiH_4^-. The optimized T_d geometries of silane, SiH_4 ($\tilde{X}\ ^1A_1$) and SiH_4^- ($\tilde{X}\ ^2A_1$) are shown in Figure 4. The three hybrid functionals predict a neutral Si−H bond length within 0.008 Å of the experimental value,[6] whereas the pure functionals overestimate experiment by nearly 0.02 Å. We also note that UCCSD(T)/aug-cc-pV5Z results give a bond length of 1.480 Å.[34]

Although SiH_4^- is predicted to have an equilibrium geometry with each functional, all functionals predict the anion to be unbound with respect to neutral SiH_4. (See Table 2.) As both CH_4 and SiH_4 have filled (Ne, Ar-like) valences, neither displays a formal electron affinity. For SiH_4, only EA_{vert} has any physical meaning, as it represents the magnitude of the temporary (picosecond) electron resonant anion state.

F. Si_2 and Si_2^-. Our optimized geometries for Si_2 ($X\ ^3\Sigma_g^-$) and Si_2^- ($X\ ^2\Sigma^+_g$) are shown in Figure 5. The geometry closest to experiment for the bond length was at the BHLYP level of theory, which was 0.003 Å longer than Huber and Herzberg's value.[65] Other functionals overestimate experiment by at least 0.025 Å, and even the UCCSD(T)/aug-cc-pV6Z result[34] overestimates by 0.006 Å. For the anion, the bond length shortens over that of the neutral as the electronic configuration changes from a $\sigma_g^2\Pi_u^2$ configuration to a $\Pi_u^4\sigma_g$ configuration, which corresponds to a $X\ ^2\Sigma_g^+$ state. The $^2\Pi_u$ state arising from a $\Pi_u^3\sigma_g^2$ configuration is known from experiment[10−12] to lie just 0.025 eV higher. Our predicted bond lengths for the anion are in reasonable agreement with experimental value $r_e = 2.127$ Å

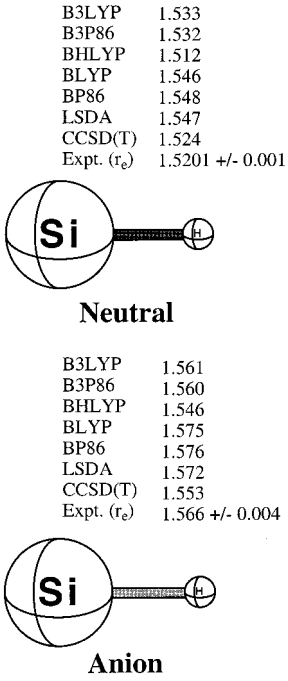

Figure 1. The molecular geometries for the X $^2\Pi$ state of SiH and the X $^3\Sigma^-$ state of SiH^-. Bond lengths are in angstroms. All results were obtained with the DZP^{++} basis set. Experimental r_e results for SiH and SiH^- are from refs 65 and 66, respectively.

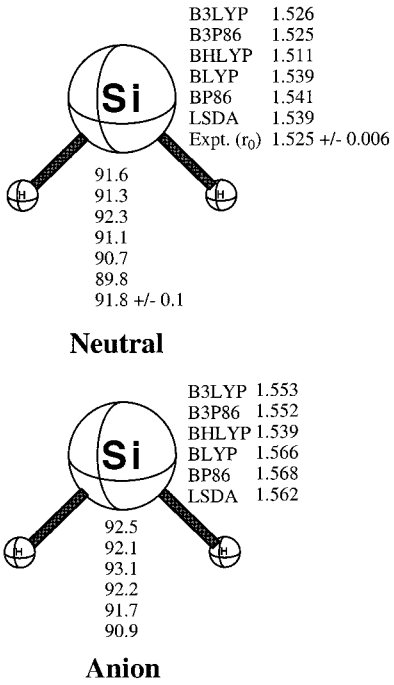

Figure 2. The molecular geometries for the $\tilde{X}\ ^1A_1$ state of SiH_2 and the $\tilde{X}\ ^2B_1$ state of SiH_2^-. Bond lengths and bond angles are in angstroms and degrees, respectively. All results were obtained with the DZP^{++} basis set. Experimental r_0 results are from ref 70.

for $^2\Sigma_g^+$ as given by Nimlos, Harding and Ellison.[15] This is also similar to $r_e = 2.1104$ Å as derived by Liu and Davies.[11,12]

Our predicted EA_{ad} values for Si_2 ranged from 1.79 to 2.90 eV, among which the BHLYP predicts the smallest (1.79 eV). The EA_{zero} value predicted by BP86 was 0.07 eV larger than the experimental value: 2.202 ± 0.01 eV.[10,15,16] Our DFT results are within 0.23 eV of experiment for this system with BP86, BLYP, and B3LYP. We also note the QCISD(T)/17s,6p,3d,1f

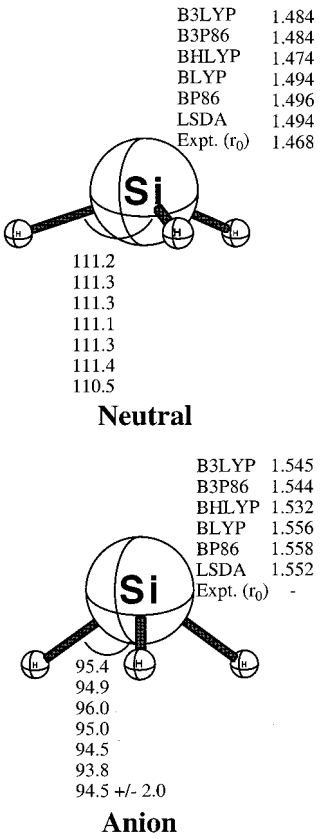

Figure 3. The molecular geometries for the $\tilde{X}\ ^2A_1$ state of SiH_3 and the $\tilde{X}\ ^1A_1$ state of SiH_3^-. Bond lengths and bond angles are in angstroms and degrees, respectively. All results were obtained with the DZP^{++} basis set. Experimental r_0 results for SiH_3 is from ref 72, and for SiH^{3-} from ref 7.

value EA = 2.09 eV as obtained by Raghavachari and Rohlfing.[18]

The σ_g and π_u molecular orbitals in the C_2 molecule are extremely close in energy and give rise to two nearly degenerate states: $^3\Pi_u$ and $^1\Sigma_g^+$, with the latter being the ground[65] state by only 716 cm^{-1}. Like many traditional ab initio methods, density functional theory has difficulties in describing ground-state C_2.[47,75−77] Indeed, most functionals predict the triplet state to be the ground state and result in highly spin contaminated wave functions for the singlet state. However, if one examines the electron affinities for C_2 using the contaminated singlet state results, one finds that the B3LYP, BLYP, and BP86 functionals all predict EAs[78] within 0.3 eV of the experimental value 3.269 eV.[79]

In contrast, the highest occupied π_u orbital is lower than the analogous σ_g orbital in Si_2, and gives a $^3\Sigma_g^-$ ground state in Si_2,[65] and the same three functionals give EA's within 0.23 eV of the experimental value, with wave functions that do not suffer from virtually any spin contamination effects for the neutral or anion species, despite the mere 0.025 eV X $^2\Sigma_g^+$ − A $^2\Pi_u$ splitting in the anion. Hence, despite the fact that DFT can predict EAs that are tolerable for both C_2 and Si_2, the DFT results for Si_2 appear to be more satisfying from a quantum mechanical point of view.

G. Si_2H and Si_2H^-. There are three possible structures for neutral Si_2H: linear ($D_{\infty h}$), bent (C_s), and H-bridged (C_{2v}) structures. In 1996, at the CCSD/TZ2P(f,d) level, Ma, Allinger, and Schaefer[30] predicted the lowest energy structure to be C_{2v} (bridged) with a $\tilde{X}\ ^2B_1$ state for neutral Si_2H.[30] The $\tilde{A}\ ^2A_1$ state was suggested to be just 0.07 eV higher than the $^2B_1$ state. These

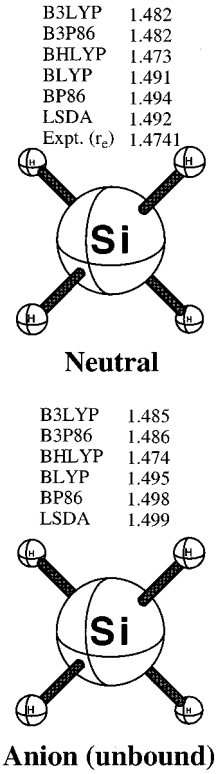

Figure 4. The molecular geometries for the $\tilde{X}\ ^1A_1$ state of SiH_4 and the unbound $\tilde{X}\ ^2A_1$ state of SiH_4^-. Bond lengths are in angstroms. All results were obtained with the DZP^{++} basis set. Experimental r_e results are from ref 6.

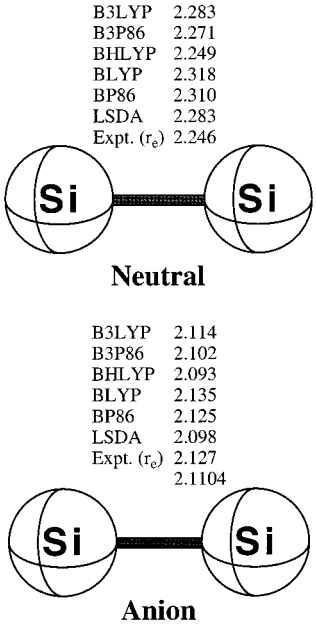

Figure 5. The molecular geometries for the $X\ ^3\Sigma_g^-$ state of Si_2 and the $X\ ^2\Sigma_g^-$ state of Si_2^-. Bond lengths are in Å. All results were obtained with the DZP^{++} basis set. Experimental r_e values for Si_2 and Si_2^- are from refs 65, 11, 12, and 15, respectively.

results were compared to the MRCI(D) results of Kalcher and Sax[27] which placed the $^2A_1$ state 0.02 eV lower than the $^2B_1$ state. Most recently, photoelectron spectroscopy experiments by Neumark and co-workers[13] and their QCISD(T)/6-31G* computations assigned the $\tilde{X}$ state to be $^2A_1$, with a 3° smaller Si−H−Si angle than the $\tilde{A}\ ^2B_1$ state, and an $\tilde{X}-\tilde{A}$ splitting of only 0.01 eV by theory and 0.020 ± 0.005 eV by experiment. It is clear that the two electronic states are essentially degenerate.

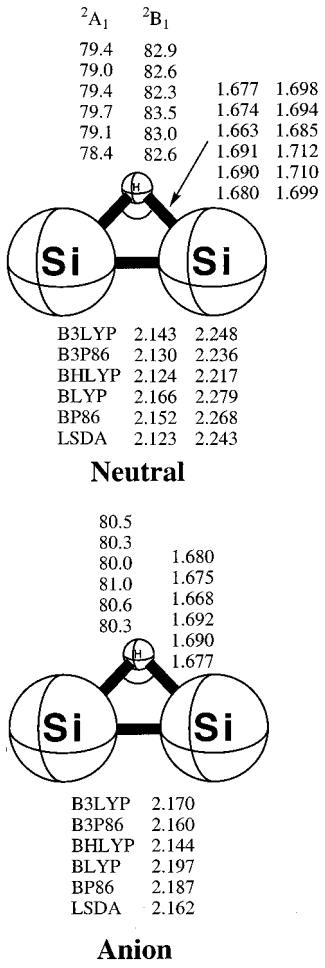

Figure 6. The molecular geometries for the $\tilde{X}\ ^2A_1$ and $\tilde{A}\ ^2B_1$ states of Si_2H and the $\tilde{X}\ ^1A_1$ state of Si_2H^-. Bond lengths and bond angles are in angstroms and degrees, respectively. All results were obtained with the DZP^{++} basis set.

Our DFT results all show the $^2A_1$ state to have a ∼3° smaller Si−H−Si angle ∼79° vs ∼82° (See Figure 6). The three hybrid functionals place the $^2B_1$ state as the ground state, by 0.008 (B3P86), 0.04 (B3LYP), and 0.12 (BHLYP) eV. While the pure functionals have the $^2A_1$ state lower by 0.0007 (BLYP), 0.04 (BP86), and 0.13 (LSDA) eV. In this work, we report results for both states. Our geometries for the neutral $^2A_1$ state are in general agreement with the QCISD(T)/6-31G* results of Neumark:[13] R_{Si-H} = 1.690 Å, r_{Si-Si} = 2.182 Å, and Si−H−Si = 80.4°. The H-bridged anion has a $^1A_1$ ground state.[27,30] To ensure that the H-bridged anion is the lowest energy Si_2H^- isomer, we optimized linear $SiSiH^-$ ($^1\Sigma^+$), which unlike neutral, linear SiSiH, does not suffer from the Renner effect, and thus remains a linear species. At the B3LYP level, without zero-point correction, we find linear $SiSiH^-$ to be 8.9 kcal/mol (0.4 eV) higher than the H-bridged anion. This is similar to results reported by Kalcher and Sax[27] of 7.3 kcal/mol using MRCI(D). Thus, both the neutral and anion species of Si_2H adopt H-bridged structures.

The B3LYP zero-point corrected adiabatic electron affinities are 2.26 eV ($^2B_1 \leftarrow {}^1A_1$) and 2.31 ($^2A_1 \leftarrow {}^1A_1$) compared to the experimental 2.31 ± 0.01 eV ($^2A_1 \leftarrow {}^1A_1$), given by photoelectron spectroscopy.[13] BP86 and BHLYP ($^2A_1 \leftarrow {}^1A_1$) EA_{zero} values are within ± 0.1 eV of experiment. (See Table 3.) The EA (CCH), which in contrast to Si_2H involves linear neutral and anion species, is larger than that for Si_2H, the former being 2.97 eV.[79]

H. Si_2H_2 and $Si_2H_2^-$. The dibridged C_{2v} or "butterfly" equilibrium geometry of disilyne, Si_2H_2 ($\tilde{X}\ ^1A_1$), and its anion,

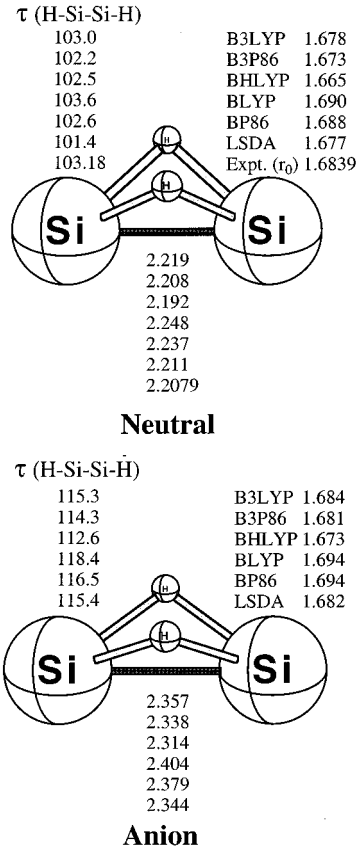

Figure 7. The molecular geometries for the $\tilde{X}\ ^1A_1$ state of dibridged Si_2H_2 and the $\tilde{X}\ ^2A_2$ state of dibridged $Si_2H_2^-$. Bond lengths and bond angles are in angstroms and degrees, respectively. All results were obtained with the DZP^{++} basis set. Experimental r_0 values are from ref 82.

$Si_2H_2^-$ ($\tilde{X}\ ^2A_2$) are shown in Figure 7. These molecules are good examples of silicon hydride molecules that show different bonding characteristics from their carbon analogues: linear acetylene, which has no formal EA. For the neutral Si_2H_2, the C_{2v} (dibridged) symmetry structure has been shown to be the most stable form.[21,26,80,81] Our hybrid DFT bond lengths for the neutral species slightly underestimate the experimental[82] Si−H distance but find good agreement for the Si−Si distance. The anion shows longer bond distances, ∼0.13 Å for Si−Si, and a ∼13° larger H−Si−Si−H torsion angle.

The predicted electron affinities for Si_2H_2 are small; our values ranged from 0.06 to 0.93 eV for the EA_{ad}. The B3LYP level of theory gives 0.45 eV for EA_{zero}, which may be representative of the true electron affinity. The experimental electron affinity is not known, as the anion ($Si_2H_2^-$) has never been detected. Our prediction of a small, but positive EA for Si_2H_2 is in contrast to the conclusion of Kalcher and Sax,[24] who state that "dibridged disilyne...is devoid of any propensity to bind an additional electron". Kalcher and Sax provide no theoretical computations to support this claim.

In 1992, Grev and Schaefer[81] examined four isomers of neutral Si_2H_2. Their work found three transition structures which allow for intramolecular isomerization between the lowest energy isomer (dibridged) and the higher lying isomers (monobridged, disilavinylidene (silyidene), and *trans*-HSiSiH). It is clear from this study that neutral Si_2H_2 will adopt a dibridged structure. Thus, the electron affinity for Si_2H_2 discussed in the proceeding paragraph assumes an adiabatic electron attachment to the neutral dibridged isomer, without further isomerization of the newly formed anion. However, many experiments, most notably photoelectron spectroscopy, measure electron affinities through detachment from the anion. Thus, we now briefly discuss other isomers of $Si_2H_2^-$, in addition to the dibridged structure shown in Figure 7.

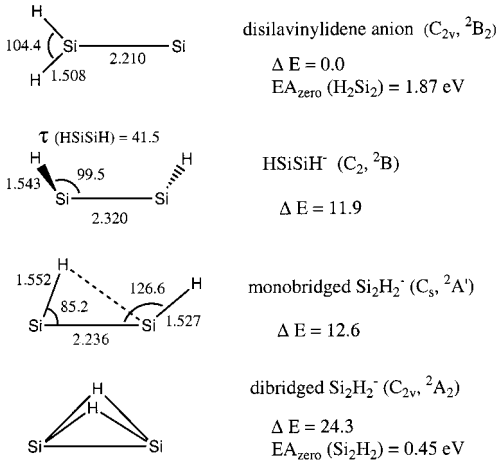

Figure 8. Four structural isomers of $Si_2H_2^-$. All results depicted are at the B3LYP level. For optimized geometries of the dibridged structure, see Figure 7. Relative energies are in kcal/mol and without ZPVE correction. Bond distances are in angstroms and angles in degrees.

In Figure 8, we show four isomers of $Si_2H_2^-$. With B3LYP, we find that the disilavinylidene anion is 24.3 kcal/mol lower than the dibridged structure, and thus represents the global minimum for $Si_2H_2^-$. Detachment from the anion to neutral disilavinylidene has an $EA_{ad} = 1.86$ eV or $EA_{zero} = 1.87$ eV. This implies that, at the B3LYP level, neutral disilavinylidene lies 10.8 kcal/mol above dibridged Si_2H_2, in good agreement with the higher level 12.3 kcal/mol value reported by Grev and Schaefer.[81] Our EA_{zero} for disiavinylidene compares well to that of Kalcher and Sax[24] who give a CEPA EA = 1.73 eV.

Thus, we have two electron affinities for Si_2H_2: EA_{zero} = 0.45 eV, representing electron attachment to the dibridged neutral, and $EA_{zero} = 1.87$ eV representing electron detachment from the disilyinylidene anion. However, in examining the dibridged $Si_2H_2^-$ anion, we encountered wave function symmetry breaking problems: the UHF solution has an imaginary b_2 harmonic frequency of 4839i cm^{-1}, with an IR intensity too large to be determined by Gaussian 94. Density functional theory is known to avoid artifactual symmetry breaking in many instances, especially when the exchange functional does not incorporate Hartree−Fock exchange.[83] Thus, it is no surprise that the magnitude of the b_2 mode changed from 4839i (UHF), 819i (BHLYP), 202i (B3LYP), to real values greater than 326 cm^{-1} for the remaining four functionals. Nonetheless, we suspect the B3LYP energetics to be relatively unaffected by the symmetry breaking and hence still recommend EA_{zero} = 0.45 eV for the dibridged neutral.

I. Si_2H_3 and $Si_2H_3^-$. In 1997, Gong, Guenzburger, and Suitovitch[33] explored five neutral Si_2H_3 isomers: two monobridged isomers, HSiHSiH (C_2) and H_2SiHSi (C_s); a dibridged isomer; a tribridged isomer; and H_3SiSi (C_s). Their ab initio molecular dynamics method found the monobridged HSiHSiH (C_2) isomer to be the lowest energy isomer, just 0.04 eV below the other monobridged isomer, 0.09 eV below the dibridged isomer, and more than 0.39 eV below the remaining two isomers. However, they did not examine the near-planar H_2SiSiH isomer (C_1). G2 results for this isomer show it to be nearly equivalent in energy to the silylsilylidyne, H_3SiSi (C_s) isomer.[23] Kalcher and Sax,[24,85] report an EA of 2.20 eV using CEPA computations between the near-planar neutral H_2SiSiH

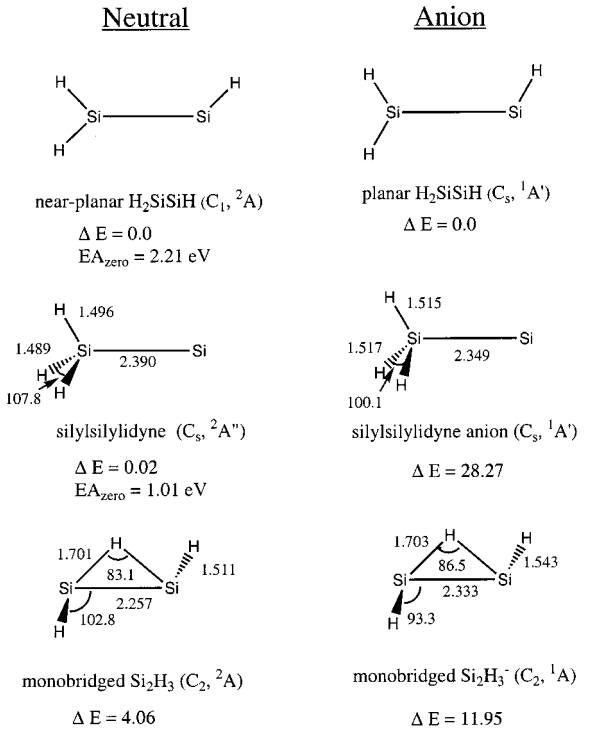

Figure 9. Three structural isomers of each Si_2H_3 and $Si_2H_3^-$. All results depicted are at the B3LYP level. For optimized geometries of the near-planar and planar H_2SiSiH/H_2SiSiH^- isomers, see Figure 10. Relative energies are in kcal/mol and without ZPVE correction. Bond distances are in angstroms and angles in degrees.

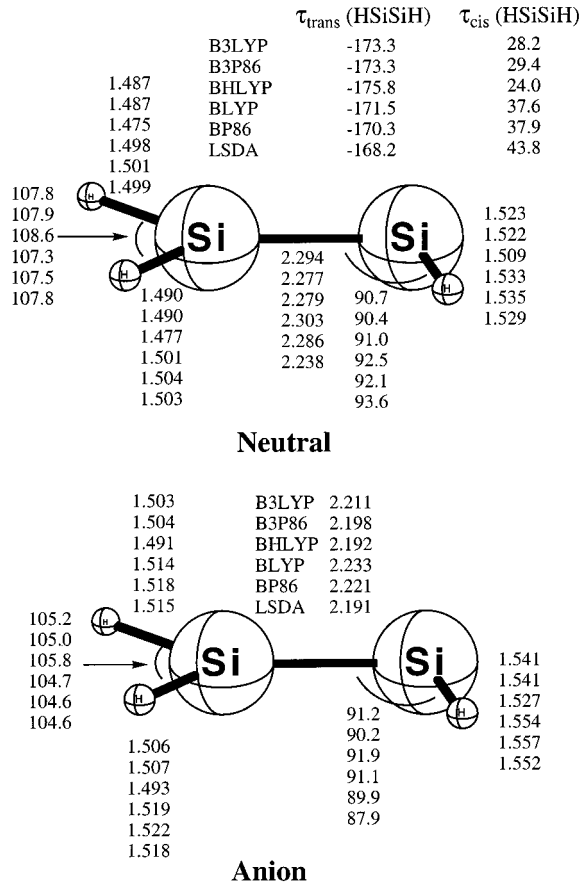

Figure 10. The molecular geometries for the $\tilde{X}\ ^2A$ state of near-planar Si_2H_3 and the $\tilde{X}\ ^1A$ state of planar $Si_2H_3^-$. Bond lengths and bond angles are in angstroms and degrees, respectively. All results were obtained with the DZP^{++} basis set.

isomer and a corresponding near-planar anion. They did not report results for other isomers.

It is beyond the scope of this paper to perform a complete investigation of all neutral and anion isomers. However, the previous results just discussed would indicate that one of monobridged HSiHSiH (C_2), near-planar H_2SiSiH (C_1), or H_3SiSi (C_s) is likely to be the neutral global minimum. In Figure 9, we show neutral and anion results for these three isomers at the B3LYP level. The near-planar C_1 isomer becomes planar with the anion and more than 11 kcal/mol more stable than the other two anion isomers. For the neutral, as first noticed by Curtiss et al.,[23] we find that the near-planar H_2SiSiH and H_3SiSi isomers are nearly equivalent in energy, the former being more stable by just 0.02 kcal/mol. Although our results at the present level of theory cannot definitively conclude which isomer is the most stable, because of the strong preference for the anion to adopt a planar H_2SiSiH^- structure we report only EA results between the planar H_2SiSiH^- isomer and the near-planar H_2SiSiH isomer with all levels of theory. At the B3LYP level only, the EA_{zero} between neutral and anion silylsilylidyne (H_3SiSi) isomers is 1.01 eV.

The near-planar (C_1) structure of Si_2H_3 ($\tilde{X}\ ^2A$) and the planar $Si_2H_3^-$ ($\tilde{X}\ ^1A'$) structures are shown in Figure 10. The most accurate adiabatic electron affinity is likely to come from the B3LYP level of theory, which gives EA_{zero} of 2.21 eV (See Table 3). Note that C_2H_3 also has a C_s, H_2CCH structure for both the neutral and anion, but has a much smaller EA = 0.667 eV.[86]

J. Si_2H_4 and $Si_2H_4^-$. From two possible C_s (silylsilylene) and C_{2h} (disilene) isomers, previous theoretical work[23,24,84] determined the lowest energy structure of neutral Si_2H_4 to be the C_{2h} isomer. Ernst, Sax, and Kalcher[84] predicted silysilylene to lie 9.1 kcal/mol above disilene with a 19.8 kcal/mol barrier for disilene to silysilylene isomerization. This is in agreement

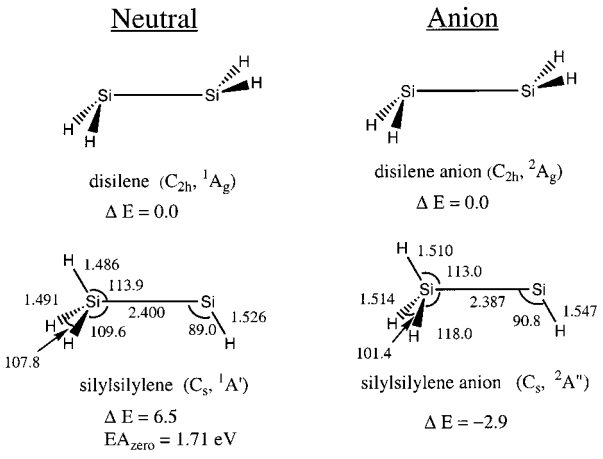

Figure 11. Two structural isomers of each Si_2H_4 and $Si_2H_4^-$. All results depicted are at the B3LYP level. For optimized geometries of the disilene isomers see Figure 12. Relative energies are in kcal/mol and without ZPVE correction. Bond distances are in angstroms and angles in degrees.

with our B3LYP results which show that disilene is 6.5 kcal/mol more stable. In the anion, we find that the silylsilylene structure (H_3SiSiH^-, C_s, $^2A''$) is slightly lower in energy than the disilene structure ($H_2SiSiH_2^-$), specifically, 2.9 and 1.7 kcal/mol with B3LYP and BP86, respectively (See Figure 11). However, because of the strong preference for the neutral species to adopt the disilene structure, we consider only the EA of disilene at all levels of theory in this present work. Our optimized disilene structures, Si_2H_4 ($\tilde{X}\ ^1A_g$) and $Si_2H_4^-$ ($\tilde{X}\ ^2A_g$)

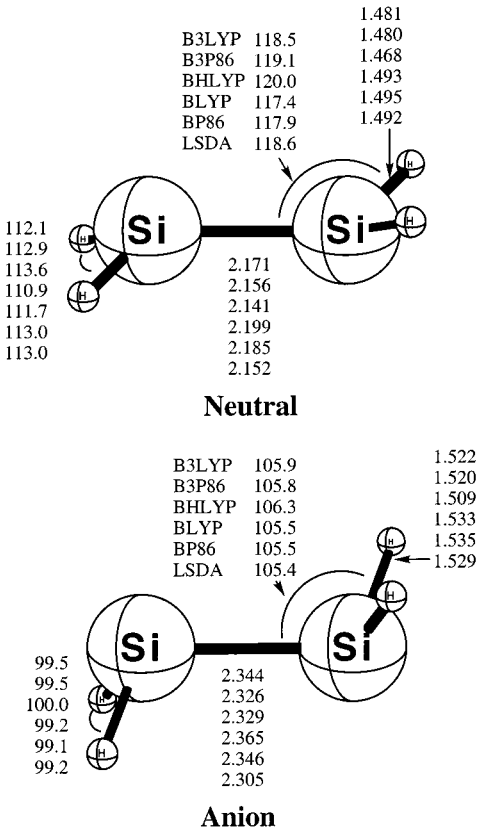

Figure 12. The molecular geometries for the $\tilde{X}\ ^1A_g$ state of Si_2H_4 and the $\tilde{X}\ ^2A_g$ state of $Si_2H_4^-$. Bond lengths and bond angles are in angstroms and degrees, respectively. All results were obtained with the DZP^{++} basis set.

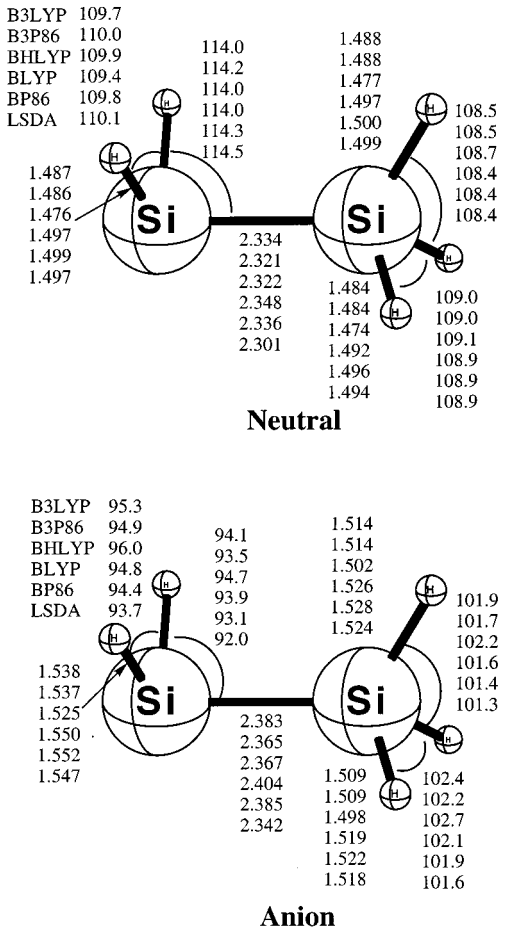

Figure 13. The molecular geometries for the $\tilde{X}\ ^2A'$ state of Si_2H_5 and the $\tilde{X}\ ^1A'$ state of $Si_2H_5^-$. Bond lengths and bond angles are in angstroms and degrees, respectively. All results were obtained with the DZP^{++} basis set.

are shown in Figure 12. The neutral and anion geometries differ significantly. In the anion, the Si−Si bond lengthens by ∼0.16 Å and the Si−Si−H angle decreases from about 118° to 105°. The $Si_2H_4^-$ anion appears to be two SiH_2 units loosely bound (Si−Si ≈ 2.33 Å) by a single electron between two overlapping b_1 orbitals. (Recall that the b_1 orbital in SiH_2 is the LUMO and is oriented perpendicular to the molecular plane). On the other hand, neutral Si_2H_4 is bound by the overlap of two filled (in-plane) a_1 orbitals from each SiH_2 unit leaving Si_2H_4 nearly planar (Si−Si ≈ 2.17 Å). For Si_2H_4, our optimized geometries agree with Curtiss et al.'s[23] MP2/6-31G* results, which give Si−Si = 2.164 Å.

In contrast to Si_2H_4, ethylene has D_{2h} symmetry. Whereas planar ethylene has no electron affinity,[87] Si_2H_4 has a rather large electron affinity, specifically, EA_{ad} = 1.28 eV at the B3LYP level of theory (see Table 3). This is similar to the B3LYP EA_{ad} for a single SiH_2 unit, 1.17 eV. The EA_{ad} values for Si_2H_4 ranged from 1.13 to 1.68 eV, 0.28 to 1.08 eV for $EA_{vert,}$ and 1.59 to 2.37 eV for VDE, which agree well with previous CEPA predictions.[24] There are no experimental electron affinities available for Si_2H_4. We predict the Si_2H_4 (disilene) electron affinity to be 1.34 eV, using our B3LYP EA_{zero} result. The EA_{zero} between neutral and anion silylsilylene (H_3SiSiH) isomers is 1.71 eV.

K. Si_2H_5 and $Si_2H_5^-$. The C_s symmetric optimized geometries of the disilyl radical, Si_2H_5 ($\tilde{X}\ ^2A'$) and $Si_2H_5^-$ ($\tilde{X}\ ^1A'$) anion are shown in Figure 13. There are no experimental results for the geometries of Si_2H_5 or $Si_2H_5^-$ or for the electron affinity of Si_2H_5. Our neutral Si_2H_5 DFT results match well with a previous optimization[23] at the MP2/6-31G* level, which gives r_{Si-Si} = 2.326 Å. Note that Si_2H_5 adopts the same C_s conformation as C_2H_5.[88]

The best adiabatic electron affinity is expected to be 1.85 eV given by B3LYP, $EA_{zero.}$ Other functionals ranged from 1.61 (BHLYP) to 2.50 eV (LSDA) for EA_{zero}, and 0.96 to 1.84 eV for EA_{vert} and 2.22 to 3.16 eV for the VDE.

L. Si_2H_6 and $Si_2H_6^-$. The D_{3d} symmetry disilane, Si_2H_6 ($\tilde{X}\ ^1A_{1g}$) and $Si_2H_6^-$ ($\tilde{X}\ ^2A_{2u}$) optimized geometries are shown in Figure 14. All of our gradient functionals overestimate the experimental bond distance extracted from Shotten, Lee, and Jones's Raman spectroscopy results.[17] The Si−Si bond distances with the BHLYP and B3P86 level of theory are only 0.005 Å longer than experiment, 2.327 Å. Our DFT average bond angle of equatorial ∠HSiH was 108.6° compared to the experimental 107.8°. Our results are close to previous UCCSD(T)/aug-cc-pVQZ results,[34] which give r_{Si-Si} = 2.346 Å, r_{Si-H} = 1.484 Å, and H−Si−H = 108.7°. The anion displays a similar geometry with a Si−Si distance which is about 0.07 Å longer. It is interesting to note that previous UHF/DZPD results[28] show that D_{3d} $Si_2H_6^-$ has two doubly degenerate imaginary frequencies and a long Si−Si bond of 3.423 Å. In contrast, all our DFT results for the D_{3d} anion show it to be a minimum with a much more reasonable Si−Si length of about 2.4 Å.

Our predicted adiabatic electron affinity for disilane is −0.61 eV (B3LYP), and unbound with each functional (see Table 3). As one might expect, there are no experimental electron affinities available, as is the case for C_2H_6, and the only relevant theoretical results are the EA_{vert}, as with SiH_4.

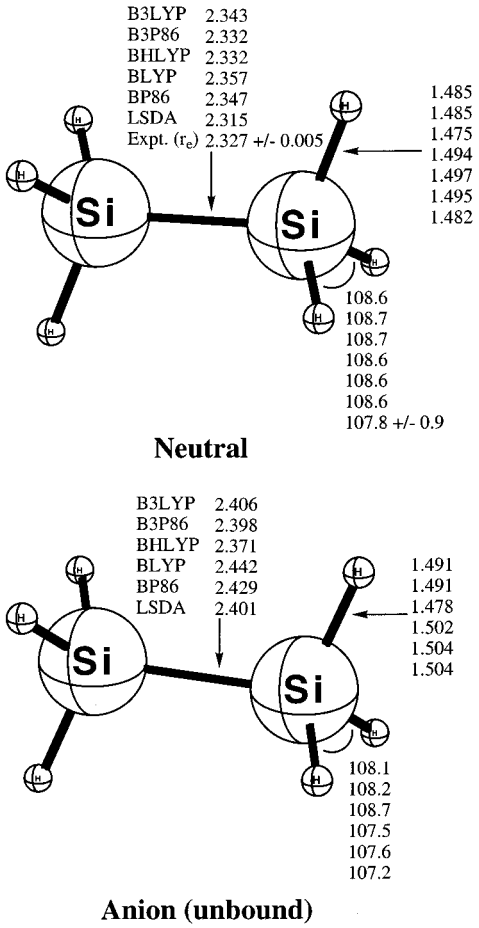

Figure 14. The molecular geometries for the $\tilde{X}\ ^1A_{1g}$ state of Si_2H_6 and the unbound $\tilde{X}\ ^2A_{2u}$ state of $Si_2H_6^-$. Bond lengths and bond angles are in angstroms and degrees, respectively. All results were obtained with the DZP^{++} basis set. Experimental r_0 values are from ref 17, but r_0(Si−H) is an assumed value.

Conclusions

On the basis of the known experimental geometries (SiH, SiH^-, SiH_2, SiH_3, SiH_4, Si_2, Si_2^-, Si_2H_4, Si_2H_6) of these systems, we conclude that the DZP^{++} BHLYP level of theory predicts the best geometries, as is the case for other inorganic species.[31,39−43] The average bond distance error with BHLYP were less than 0.01 Å, compared to all experimental values. In general, the hybrid functionals gave better results than the pure functionals; pure functionals often overestimated bond lengths, by as much as 0.02 Å in some cases.

For electron affinities, the average absolute error (EA_{zero} vs exptl) with each functional in order is B3LYP (0.06 eV) < BLYP (0.12 eV) < BP86 (0.15 eV) < BHLYP (0.19 eV) < B3P86 (0.57 eV) < LSDA (0.63 eV). The average maximum error for each functional in order is B3LYP (0.15 eV) < BLYP (0.23 eV) < BP86 (0.25 eV) < BHLYP (0.42 eV) < B3P86 (0.67 eV) < LSDA (0.69 eV). For all but BHLYP and BLYP, average absolute errors between experiment and our predicted EA_{ad} are better than those just given for EA_{zero} by 0.01−0.02 eV. Clearly, B3LYP is a superior choice for examining the electron affinities of silicon hydride systems. Using B3LYP EA_{zero} values, we predict electron affinities for dibridged Si_2H_2 (0.45 eV), Si_2H_3 (2.21 eV), disilene Si_2H_4 (1.34 eV), and the disilyl radical Si_2H_5 (1.85 eV). For disilavinylidene, Si_2H_2, we find an EA_{zero} = 1.87 eV, for silylsilylidyne, H_3SiSi an EA_{zero} = 1.01 eV, and for silylsilylene an EA_{zero} = 1.71 eV. These values are probably within 0.1 eV of the true electron affinities. It is also comforting to see that all of B3LYP, BLYP, BP86, and BHLYP methods have absolute average errors of less than 0.2 eV, despite low-lying excited states encountered in some silicon hydride systems (i.e., Si_2^- and Si_2H). It is not necessarily surprising that BHLYP predicts the best geometries but not the best electron affinities. The BHLYP functional has significant Hartree−Fock exchange which increases the method error in energy predictions, while on the other hand offsetting the density functional tendency to overestimate bond-lengths (as noted in the preceding paragraph).

Comparing the geometries and electron affinities of the silicon hydride systems to corresponding carbon analogues, shows important differences. For example, C_2H_4 and Si_2H_4 have very different bonding characteristics and show different electron affinities. The C_2H_4 has D_{2h} symmetry whereas Si_2H_4 has C_{2h} symmetry, and Si_2H_4 has an electron affinity of 1.34 eV (B3LYP) whereas ethylene has no electron affinity. Furthermore, one can see that Si_2 and C_2 have a rather large electron affinity difference, about one eV. Some analogues are similar in nature in terms of geometry and/or electron affinities: Si vs C, SiH vs CH, SiH_4 vs CH_4, Si_2H_5 vs C_2H_5, Si_2H_6 vs C_2H_6. We hope that these theoretical predictions will provide motivation for the experimental study of the lesser characterized silicon hydride systems, especially in instances such as $Si_2H_2^-$, $Si_2H_3^-$, and $Si_2H_4^-$ where the anion potential energy surface does not mirror that of the corresponding neutral species. It seems clear that DFT methods would also be useful in predictions of the electron affinities of the larger silicon hydrides, beginning with the Si_3H_x series.

Acknowledgment. This work is supported by the U.S. National Science Foundation Grant CHE-9815397. C.H.P. thanks Brian Hoffman for his help in the beginning stage of this work. J.C.R.K. thanks Christine Rienstra-Kiracofe for research assistance.

Appendix

After submission of this manuscript, electron affinity computations of Si_xH_y molecules were published by M. T. Swihart [*J. Phys. Chem.* **2000**, *104*, 6083]. Although Swihart focuses on larger SixHy compounds, he presents briefly B3LYP/6-311+G(3df,2p)//B3LYP/6-31G(d) results for Si, SiH, SiH_2, SiH_3, Si_2, Si_2H, Si_2H_4 (both H_3SiSiH and H_2SiSiH_2) and Si_2H_5 which are within 0.1 eV of our computed B3LYP/DZP^{++} results. Comparison of geometries are not possible because structures are not given by Swihart; however, Swihart notes geometric changes between the neutral and anion species of H_2SiSiH_2 and H_3SiSiH_2 which are nearly identical to our results. Swihart does not provide EAs for Si_2H_2 or Si_2H_3, or any EA_{vert} or VDE energies. Swihart does not specify which state of Si_2H was used for his Si_2H EA. Swihart's paper complements this present work by investigating electron affinities of larger silicon hydrides, and we encourage interested readers to consults both papers.

References and Notes

(1) Lickiss, P. D. In *Encyclopedia of Inorganic Chemistry*; King, R. B., Ed.; John Wiley & Sons: Chichester, 1994; Vol. 7, 3770.
(2) Jasinski, J. M.; Meyerson, B. S.; Scott, B. A. *Annu. Rev. Phys. Chem.* **1987**, *38*, 109.
(3) Dubois, I. *Can. J. Phys.* **1968**, *46*, 2485.
(4) Kasdan, A.; Herbst, E.; Lineberger, W. C. *J. Chem. Phys.* **1975**, *62*, 541.
(5) Brown, J. M.; Robinson, D. *Mol. Phys.* **1984**, *51*, 883.
(6) Ohno, K.; Matsuura, H.; Endo, Y.; Hirota, E. *J. Mol. Spectrosc.* **1985**, *111*, 73.
(7) Nimlos, M. R.; Ellison, G. B. *J. Am. Chem. Soc.* **1986**, *108*, 6522.

(8) Boo, B. H.; Armentrout, P. B. *J. Am. Chem. Soc.* **1987**, *109*, 3549.
(9) Berkowitz, J.; Greene, J. P.; Cho, H.; Ruščić, B. *J. Chem. Phys.* **1987**, *86*, 1235.
(10) Arnold, C. C.; Kitsopoulos, T. N.; Neumark, D. M. *J. Chem. Phys.* **1993**, *99*, 766.
(11) Liu, Z.; Davies, P. B. *Phys. Rev. Lett.* **1996**, *76*, 596.
(12) Liu, Z.; Davies, P. B. *J. Chem. Phys.* **1996**, *105*, 3443.
(13) Xu, C.; Taylor, T. R.; Burton, G. R.; Neumark, D. M. *J. Chem. Phys.* **1998**, *108*, 7645.
(14) Scheer, M.; Bilodeau, R. C.; Brodie, C. A.; Haugen, H. K. *Phys. Rev. A.* **1998**, *58*, 2844.
(15) Nimlos, M. R.; Harding, L. B.; Ellison, G. B. *J. Chem. Phys.* **1987**, *87*, 5116.
(16) Kitsopoulos, T. N.; Chick, C. J.; Zhao, Y.; Neumark, D. M. *J. Chem. Phys.* **1991**, *95*, 1441.
(17) Shotten, K. C.; Lee, A. G.; Jones, W. J. *J. Raman Spectrosc.* **1973**, *1*, 243.
(18) Raghavachari, K.; Rohlfing, C. M. *J. Chem. Phys.* **1991**, *94*, 3670.
(19) Viswanathan, R.; Thompson, D. L.; Raff, L. M. *J. Chem. Phys.* **1984**, *80*, 4230.
(20) Allen, W. D.; Schaefer, H. F. *Chem. Phys.* **1986**, *108*, 243.
(21) Colegrove, B. T.; Schaefer, H. F. *J. Phys. Chem.* **1990**, *94*, 5593.
(22) Shen, M.; Schaefer, H. F. *Mol. Phys.* **1992**, *76*, 467.
(23) Curtiss, L. A.; Raghavachari, K.; Deutsch, P. W.; Pople, J. A. *J. Chem. Phys.* **1991**, *95*, 2433.
(24) Kalcher, J.; Sax, A. F. *Chem. Phys. Lett.* **1992**, *192*, 451.
(25) Becerra, R.; Walsh, R. *J. Phys. Chem.* **1992**, *96*, 10856.
(26) Hühn, M. M.; Amos, R. D.; Kobayashi, R.; Handy, N. C. *J. Chem. Phys.* **1993**, *98*, 7107.
(27) Kalcher, J.; Sax, A. F. *Chem. Phys. Lett.* **1993**, *215*, 601.
(28) Tada, T.; Yoshimura, R. *J. Phys. Chem.* **1993**, *97*, 1019.
(29) Taketsugu, T.; Gordon, M. S. *J. Phys. Chem.* **1995**, *99*, 8462.
(30) Ma, B.; Allinger, N. L.; Schaefer, H. F. *J. Chem. Phys.* **1996**, *105*, 5731.
(31) King, R. A.; Mastryukov, V. S.; Schaefer, H. F. *J. Chem. Phys.* **1996**, *105*, 6880.
(32) Yamaguchi, Y.; Van Huis, T. J.; Sherrill, C. D.; Schaefer, H. F. *Theor. Chem. Acc.* **1997**, *97*, 341.
(33) Gong, X. G.; Guenzburger, D.; Saitovitch, E. B. *Chem. Phys. Lett.* **1997**, *275*, 392.
(34) Feller, D.; Dixon, D. A. *J. Phys. Chem.* **1999**, *103*, 6413.
(35) Jursic, B. S. *J. Mol. Struct.* (*THEOCHEM*) **2000**, *497*, 65.
(36) Aarset, K.; Császár, A. G.; Sibert, E. L.; Allen, W. D.; Schaefer, H. F.; Klopper, W.; Noga, J. *J. Chem. Phys.* **2000**, *112*, 4053.
(37) Kutzelnigg, W. *Angew. Chem., Int. Ed. Engl.* **1984**, *23*, 272.
(38) Sannigrahi, A. B.; Nandi, P. K. **1992**, *188*, 575.
(39) King, R. A.; Galbraith, J. M.; Schaefer, H. F. *J. Phys. Chem.* **1996**, *100*, 6061.
(40) Tschumper, G. S.; Fermann, J. T.; Schaefer, H. F. *J. Chem. Phys.* **1996**, *104*, 3676.
(41) Van Huis, T. J.; Galbraith, J. M.; Schaefer, H. F. *Mol. Phys.* **1996**, *89*, 607.
(42) King, R. A.; Pettigrew, N. D.; Schaefer, H. F. *J. Chem. Phys.* **1997**, *107*, 8536.
(43) Pak, C.; Xie, Y.; Van Huis, T. J.; Schaefer, H. F. *J. Am. Chem. Soc.* **1998**, *120*, 11115.
(44) Brinkmann, N. R.; Tschumper, G. S.; Schaefer, H. F. *J. Chem. Phys.* **1999**, *110*, 6240.
(45) Brown, S. T.; Rienstra-Kiracofe, J. C.; Schaefer, H. F. *J. Phys. Chem. A.* **1999**, *103*, 4065.
(46) Rienstra-Kiracofe, J. C.; Graham, D. D.; Schaefer, H. F. *Mol. Phys.* **1998**, *94*, 767.
(47) Tschumper, G. S.; Schaefer, H. F. *J. Chem. Phys.* **1997**, *107*, 2529.
(48) Becke, A. D. *Phys. Rev. A.* **1988**, *38*, 3098.
(49) Lee, C.; Yang, W.; Parr, R. G. *Phys. Rev. B.* **1988**, *37*, 785.
(50) Becke, A. D. *J. Chem. Phys.* **1993**, *98*, 1372.
(51) Becke, A. D. *J. Chem. Phys.* **1993**, *98*, 5648.
(52) Perdew, J. P. *Phys. Rev. B.* **1986**, *33*, 8822; *34*, 7046.
(53) Vosko, S. H.; Wilk, L.; Nusair, M. *Can. J. Phys.* **1980**, *58*, 1200.
(54) Slater, J. C. *Quantum Theory of Molecular and Solids: The Self-Consistent Field for Molecular and Solids*; McGraw-Hill: New York, 1974; Vol. IV.
(55) Kohn, W.; Sham, L. J. *Phys. Rev A.* **1965**, *140*, 1133.
(56) Frisch, M. J.; Trucks, G. W.; Schlegel, H. B.; Gill, P. M. W.; Johnson, B. G.; Robb, M. A.; Cheeseman, J. R.; Keith, T. A.; Petersson, G. A.; Montgomery, J. A.; Raghavachari, K.; Al-Laham, M. A.; Zakrzewski, V. G.; Ortiz, J. V.; Foresman, J. B.; Cioslowski, J.; Stefanov, B. B.; Nanayakkara, A.; Challacombe, M.; Peng, C. Y.; Ayala, P. Y.; Chen, W.; Wong, M. W.; Andres, J. L.; Replogle, E. S.; Gomperts, R.; Martin, R. L.; Fox, D. J.; Binkley, J. S.; Defrees, D. J.; Baker, J.; Stewart, J. P.; Head-Gordon, M.; Gonzalez, C.; Pople, J. A. GAUSSIAN 94, Revision C.3, Gaussian, Inc.: Pittsburgh, PA, 1995.
(57) Huzinaga, S. *J. Chem. Phys.* **1965**, *42*, 1293. Dunning, T. H. *J. Chem. Phys.* **1970**, *53*, 2823; *Approximate Atomic Wave functions II*, Department of Chemistry Report; University of Alberta: Edmonton, Alberta, Canada, 1971. Dunning, T. H.; Hay, P. J. *Modern Theoretical Chemistry*; Schaefer, H. F., Ed.; Plenum: New York, 1977; Vol. 3, pp 1−27.
(58) Lee, T. J.; Schaefer, H. F. *J. Chem. Phys.* **1985**, *83*, 1784.
(59) Rittby, M.; Bartlett, R. J. *J. Phys. Chem.* **1988**, *92*, 3033.
(60) Watts, J. D.; Gauss, J.; Barlett, R. J. *J. Chem. Phys. Lett.* **1992**, *200*, 1.
(61) Watts, J. D.; Gauss, J.; Barlett, R. J. *J. Chem. Phys.* **1993**, *98*, 8718.
(62) Dunning, T. H. *J. Chem. Phys.* **1989**, *90*, 1007.
(63) Woon, D. E.; Dunning, T. H. *J. Chem. Phys.* **1993**, *98*, 1358.
(64) ACES II is a program product of the Quantum Theory Project, University of Florida. Stanton, J. F.; Gauss, J.; Watts, J. D.; Nooijen, M.; Oliphant, N.; Perera, S. A.; Szalay, P. G.; Lauderdale, W. J.; Gwaltney, S. R.; Beck, S.; Balkova, A.; Bernholdt, D. E.; Baeck, K.-K.; Rozyczko, P.; Sekino, H.; Hober, C.; Barlett, R. J. Integral packages included are VMOL (Almlof, J.; Taylor, P. R.); VPROPS (Taylor, P.); ABACUS (Helgaker, T.; Jensen, H. J. Aa.; Jorgensen, P.; Olsen, J.; Taylor, P. R.).
(65) Huber, K. P.; Herzberg, G. *Molecular Spectra and Molecular Structure, Constants of Diatomic Molecules*; Van Nostrand Reinhold: New York, 1979; Vol. IV.
(66) Rosmus, P.; Meyer, W. *J. Chem. Phys.* **1978**, *69*, 2745.
(67) Lewerenz, M.; Bruna, P. J.; Peyerimhoff, S. D.; Buenker, R. J. *J. Phys. B.* **1983**, *16*, 4511.
(68) Kalcher, J. *Chem. Phys.* **1987**, *118*, 273.
(69) Kasdan, A.; Herbst, E.; Lineberger, W. C. *Chem. Phys. Lett.* **1975**, *31*, 78.
(70) Yamada, C.; Kanamori, H.; Hirota, E.; Nishiwaki, N.; Itabashi, N.; Kato, K.; Goto, T. *J. Chem. Phys.* **1989**, *91*, 4582.
(71) Leopold, D. G.; Murray, K. K.; Miller, A. E. S.; Lineberger, W. C. *J. Chem. Phys.* **1985**, *83*, 4849.
(72) Yamada, C.; Hirota, E. *Phys. Rev. Lett.* **1986**, *56*, 923.
(73) Ellison, G. B.; Engelking, P. C.; Lineberger, W. C. *J. Am. Chem. Soc.* **1978**, *100*, 2556.
(74) Tschumper, G. S.; Rienstra-Kiracofe, J. C.; Barden, C. J.; Brown, S. T.; Schaefer, H. F. Work in progress.
(75) Hutter, J.; Lüthi, H. P.; Diederich, F. *J. Am. Chem. Soc.* **1994**, *116*, 750.
(76) Curtiss, L. A.; Redfern, P. C.; Raghavachari, K.; Pople, J. A. *J. Chem. Phys.* **1998**, *109*, 42.
(77) Miller, T. F.; Hall, M. B. *J. Am. Chem. Soc.* **1999**, *121*, 7389.
(78) Tschumper, G. S. Unpublished results.
(79) Ervin, K. M.; Lineberger, W. C. *J. Phys. Chem.* **1991**, *95*, 1167.
(80) Lischka, H.; Köhler, H. *J. Am. Chem. Soc.* **1983**, *105*, 6646.
(81) Grev, R. S.; Schaefer, H. F. *J. Chem. Phys.* **1992**, *97*, 7990.
(82) Bogey, M.; Bolvin, H.; Demuynck, C.; Destombes, J. L. *Phys. Rev. Lett.* **1991**, *66*, 413.
(83) Sherrill, C. D.; Lee, M. S.; Head-Gordon, M. *Chem. Phys. Lett.* **1999**, *302*, 425.
(84) Ernst, M. C.; Sax, A. F.; Kalcher, J. *Chem. Phys. Lett.* **1993**, *216*, 189.
(85) Sax, A. F.; Kalcher, J. *J. Mol. Struct.* (*THEOCHEM*) **1990**, *208*, 123.
(86) Ervin, K. M.; Gronert, S.; Barlow, S. E.; Gilles, M. K.; Harrison, A. G.; Bierbaum, V. M.; DePuy, C. H.; Linegerger, W. C.; Ellison, G. B. *J. Am. Chem. Soc.* **1990**, *112*, 5750.
(87) Burrow, P. D.; Jordan, K. D. *Chem. Phys. Lett.* **1975**, *36*, 594.
(88) Wong, M. W.; Baker, J.; Nobes, R. H.; Radom, L. *J. Am. Chem. Soc.* **1987**, *109*, 2245.